

ACTIVE TECTONICS IN TAIWAN FROM INSAR TECHNIQUES

PI 112

B. Deffontaines¹, E. Pathier², B. Fruneau¹, J.-C. Hu³, J. Champenois¹, K.-C. Lin³

¹ GTMC, Université Paris-Est, Marne-la-Vallée, 77454, France.

² ISTerre, Université Joseph Fourier, Grenoble, 38041, France.

³ Department of Geosciences, National Taiwan University, Taipei, Taiwan.

1. INTRODUCTION

The aim of this three years project was to use the new ALOS data to improve strain measurement related to active faulting in Taiwan. The main objective of this study is to understand processes between major earthquakes (during interseismic period), that leads to slow and subtle deformations, in order to better understand seismic cycle. During the interseismic phase of the cycle, stress builds up causing aseismic slip on some portions of faults (up to several centimeters per year) and also distributed deformation that is in part elastic (this part that will be released during the quake). The related surface displacements are more subtle than those of major earthquakes, however, they can be observed over longer time. It is fundamental to measure and analyze such surface displacements which are important sources of information about the geometry, average slip rate and spatial and temporal slip distribution on fault.

For this kind of monitoring, we decided to use both Differential SAR Interferometry (D-INSAR) and new interferometric approaches, which are better adapted to small deformations measurement: “Small Baseline” [1] and “Persistent Scatterers” [2,3] approaches. Our analysis goes with GPS and field investigations.

Located at the boundary of two tectonic plates converging at a rate of 8.2 cm per year [4] (Fig. 1), Taiwan is one of the most deforming areas in the world. The specificity of Taiwan is that it concentrates over a relatively small area (140 km by 370 km) a large range of tectonic processes that can be observed in a short time-scale (~3 years). Another interest of such area is the high frequency of earthquakes. Another reason to choose Taiwan is the availability of GPS and seismological networks that are amongst the densest in the world.

Active faulting phenomena are important issues in Taiwan, as all human activity are sensitive to earthquake.

As no major earthquakes ($M > 6$) occurred on our areas of study during the last three years (2007-2011), we concentrated on the interseismic phase.

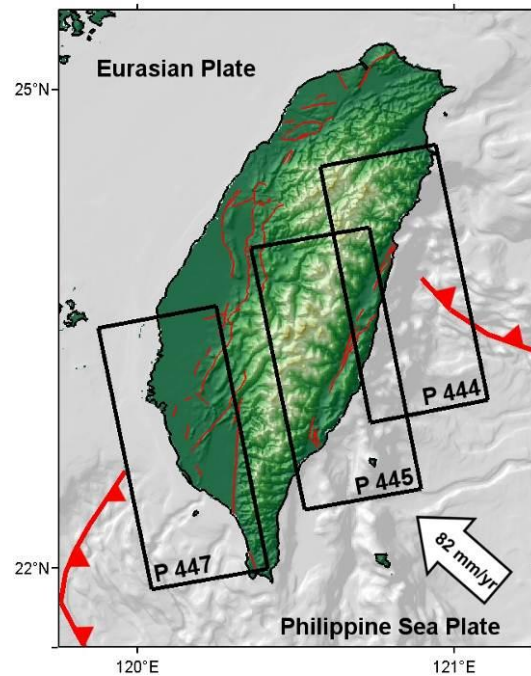


Fig. 1 Map of Taiwan and ALOS PALSAR paths used for this study. Red thickness lines represent the suture plate boundaries while red narrow lines show active faults from Central Geological Survey Taiwan (CGS).

We have chosen two major active areas for monitoring interseismic deformation by applying both DInSAR and PS-InSAR. The first one is the Longitudinal Valley (Fig. 2A), located in the eastern part of Taiwan, where aseismic creep has been monitored with GPS networks [5], leveling campaigns [6], creepmeters [7] and more recently with interferometric methods using ERS SAR data in C-band [8].

The second area of interest is composed by Tainan, Kaohsiung and Pingtung in the South West of Taiwan (Fig. 2B). Several studies using GPS and DInSAR were published on the monitoring of the active anticline of Tainan [9,10] and the subsidence of Pingtung plain [11]. However, variations of interseismic deformations seem to have occurred after the disastrous 21th September Chi-Chi earthquake.

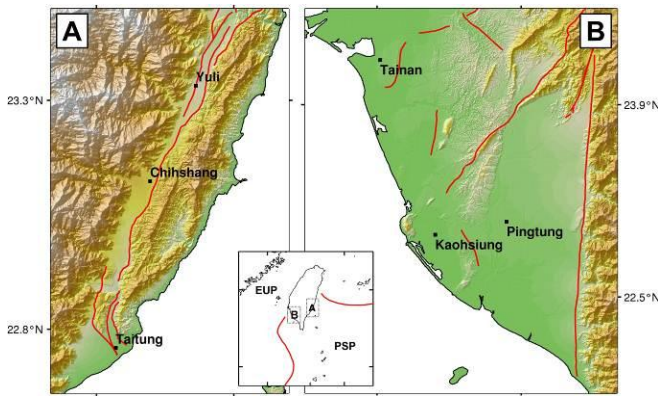


Fig. 2 Map of active faults for the two studied areas (CGS). (A) The Longitudinal Valley, Eastern Taiwan. (B) South West of Taiwan.

2. METHOD

During the interseismic period, aseismic slip and distributed deformation occur. Those deformations can be measured by GPS networks since the 90's. However, due to the complex geodynamical context of Taiwan and high strain rate, the pattern of deformation is complex, and is not well solved by current GPS networks. In complement, DInSAR, with its high spatial resolution, has been shown to provide useful information in active areas of Taiwan. InSAR has been successfully applied to study large earthquake in Taiwan [12]. Other DInSAR studies have also shown in some part of the Island the feasibility and the high interest of interferometry in measuring strain [8,9,10,13]. In the Tainan area (SW Taiwan), we have revealed, using SAR images from ERS satellite, interseismic and aseismic slow tectonic motion occurring on an active geological structure delimited by faults [9].

In that study, we measure and monitor interseismic deformations using different interferometric methods, combined with GPS data. While previous studies used ERS SAR data in C-band, we take advantages of the L-Band of PALSAR which are more penetrative and thus more convenient in area of luxuriant vegetation like in Taiwan.

2.1 Differential Interferometry Radar

First, we used DInSAR, which is an efficient technique for measuring crustal deformation [14,15] and had been previously used in Taiwan with success over quite urbanized area [9,16]. It is based on phase difference between two SAR images acquired at different times over the same area. The resulting interferometric phase is then corrected from the orbital and topographic components (using the precise knowledge orbits and the use of a 40 meters Digital Elevation Model) in order to finally obtain a differential interferogram mapping the surface deformation in the Line of Sight radar direction, between the two acquisitions. However, it is polluted by some

potential DEM errors, and cumbersome atmospheric artifacts, due to the propagation delays of the radar wave through the atmosphere, those last ones being difficult to eliminate totally.

The quality of an interferogram principally depends on coherence, decreasing with perpendicular and temporal baselines between satellite passes. All interferograms are processed with the Repeat Orbit Interferometry Package (ROI_PAC) [17].

In the whole dataset, numerous interferograms present a low coherence and some atmospheric artifacts, preventing to use them to extract properly deformation signal.

2.2 Time series analysis

To overcome all these limits, new recent techniques based on the identification and the study of stable radar targets also called "Persistent Scatterers", have been developed. Those techniques allow to measure, in area with low global coherence, displacement on specific points (PS), which correspond to strongly reflecting targets, with a phase stable over long period of time, and for varying viewing angles. These multi-images techniques allow also to cope with atmospheric artifacts (the second limitation of DInSAR), and then improve accuracy of displacement measurement. We have used time series analysis through "Persistent Scatterers" method developed by Andy Hooper at University of Delft, called Stanford Method for Persistent Scatterers (StaMPS) [3]. This software uses both information of phase stability and amplitude dispersion with time to determine which pixel can be considered as Persistent Scatterers.

Firstly, an important step consists on the choice of the "Super Master" image which will be used to coregister all images in the same geometry and to form the series of interferograms according to this same reference. This step is determinant for the continuation of the processing: this image is chosen in order to minimize spatial and temporal decorrelation [18]. Later, DORIS software [19] is used to calculate all the interferograms and to correct the interferometric phase from flatten earth and topographic terms (with 40 meters DEM). Finally, after these steps, all pixels of interferograms are geocoded into the DEM coordinate system.

The StaMPS specific process can then be applied on the series of differential interferograms previously generated. It is composed by three main stages. The first one is the extraction of a subset of PS candidates (PSC pixels) using their amplitude dispersion index [2] (threshold value is usually fixed to 0.4). However, a fraction of the selected pixel candidates are not really PS and will be eliminated at the end of the process. The second step starts with an iterative process which estimates the phase stability of each PSC. By combining both amplitude dispersion with the criterion of phase stability previously estimated, PSC which appear to be not

true PS are excluded until the end of the process. Consequently, all interferograms are unwrapped using SNAPHU software [20].

Next, in order to try to remove atmospheric term of unwrapped phases, a high pass filter in time and a low-pass filter in space are sequentially applied to estimate spatially correlated noises from respectively “Super Master” and slave images.

At the end, we obtain a map of mean displacement in radar Line Of Sight (LOS) showing the aseismic slip on the whole period of study, for all PS. It is also possible to reconstruct the time series of displacement from the StaMP’s output files, in order to have access to the temporal evolution of each PS, with a measure of displacement for each acquisition date.

3. LONGITUDINAL VALLEY

The Longitudinal Valley (LV), in the Eastern Taiwan, is one of the suture plate boundaries of the active collision between the EUP and the PSP (Fig. 2A). About 30% of the total convergence is relaxed along its 150 km length. An important historical seismicity is observed in this Valley, with a series of five large earthquakes ($M > 7$) in autumn 1951 [21], and more recently the $M_w = 6.5$ Chengkung earthquake [22]. This significant activity is due to the Longitudinal Valley Fault (LVF) which is one of the most active structures of Taiwan with a 3 cm/yr mean horizontal shortening rate [5]. The LVF is a thrust fault with a minor left-lateral component, trends $N20^\circ E$ and dips $39-45^\circ$ to the east [8].

In this area, 70 images acquired along two paths (444 for the northern part and 445 for the southern part) and corresponding to 2 different frames have been ordered (Fig. 1). But we decided to focus only on the south of the LV, the most active segment of the LVF.

More than 20 interferograms were processed. Two particular interferograms (Fig. 3) show a clear signal of deformation located in the Longitudinal Valley that we considered as the location of the major LVF trace. These interferograms present a high coherence due to their very low perpendicular baseline (less than 70 meters) but also thanks to L-Band, which is favorable for interferometric study on such area of luxuriant vegetation. The temporal baseline is 920 days between master and slave images, which is large enough to detect and extract signal of deformation. A clear discontinuity is present on both interferograms with a change of color (from blue to red) separating two blocks with different behaviors: the uplifting eastern block corresponding to the Coastal Range and the western stable block composed by the Central Range and the Longitudinal Valley. One cycle of color from blue to red corresponds to a displacement of $\lambda/2$ (11.8 cm) toward the satellite. From these first results, we have updated existing previous fault map [21], improving the precision of localization of fault line.

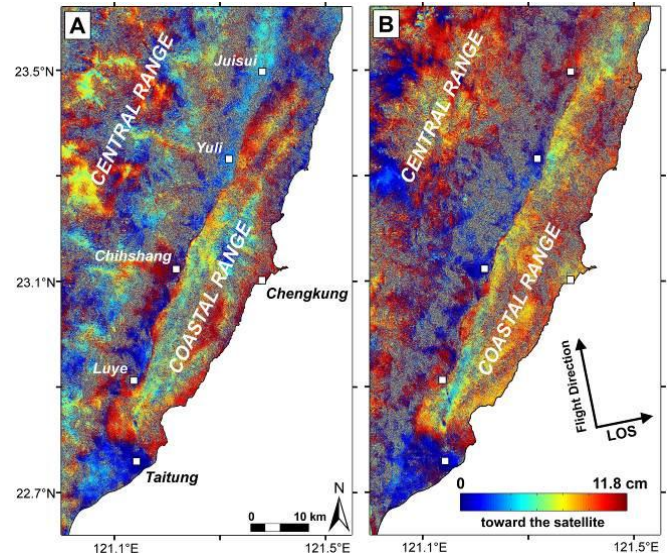


Fig. 3 ALOS PALSAR Differential Interferograms. (A) Differential interferogram 29.01.2007 - 06.08.2009 with a -68m perpendicular baseline. (B) Differential interferograms 01.08.2007-06.02.2010 with a 43m perpendicular baseline.

The interferograms presented in Figure 3 are very coherent, but in the whole stack of generated interferograms, numerous are affected by atmospheric artifacts and/or present very low coherence even with small perpendicular baseline. It is then difficult to extract signal deformation without significant errors and retrieve also time series analysis of the deformation, allowing temporal evolution analysis.

To overcome these problems, we used StaMPS software. 10 PALSAR images were processed to generate 9 interferograms with the September 16th 2007 image as “Super Master” reference. Perpendicular baselines are between 1400 m and -1100 m which are more than reasonable values for L-band ALOS PALSAR data. We chose a 0.4 threshold value for amplitude dispersion and a criterion of 15% for maximum noisiest pixels of the starting subset of PSC. StaMPS needs a reference to determine absolute displacement values, so we chose the city of Yuli as reference. At the end of processing, we obtain a total of 77 133 PS over the last 90 kilometers of the Longitudinal Valley.

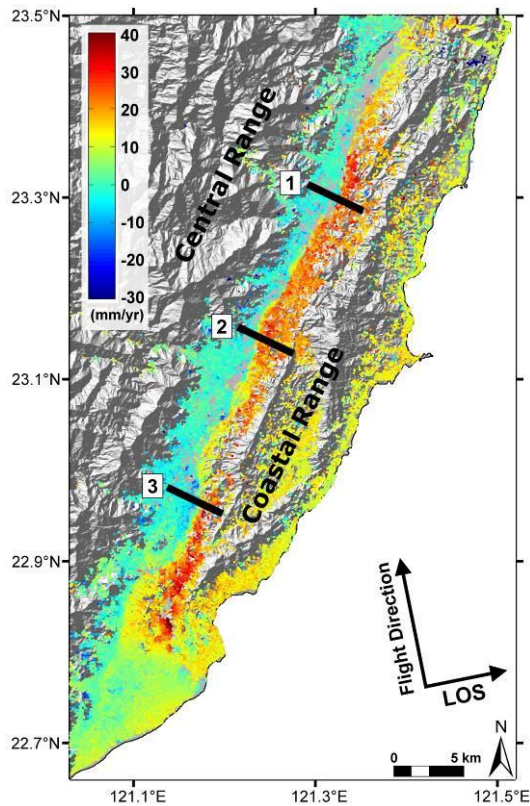


Fig. 4 PS-InSAR map of mean displacement using L-band PALSAR data obtained with StaMPS (January 2007 – February 2010). The three black lines indicate the location of the profiles presented in Fig. 5.

Figure 4 shows the map of mean LOS velocity obtained with StaMPS for the period between January 2007 and February 2010. We distinguish two different domains: the south ending of the Valley, near Taitung city, where the PS density is higher than 55 PS/km², and the rest of the valley where, on contrary, PS density is about 40 PS/km². This difference is due to large urbanization in the south valley while the other part of the valley is mainly occupied by farming.

As it was observed on DInSAR results, we have two areas with different displacements separated by the LVF. PS-InSAR results highlight the aseismic creep of the Longitudinal Valley Fault. They confirm the uplift of the Coastal Range and the quasi stability of the valley with the Central Range according to the Yuli reference area. This new map of surface deformation allows us to modify and increase the precision of the fault trace we obtained with our DInSAR results.

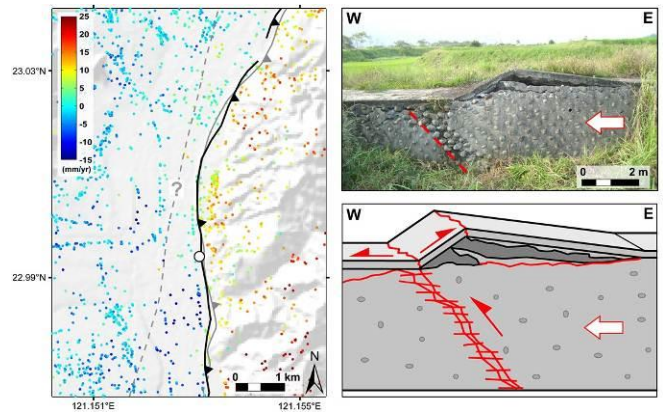


Fig. 5 PS-InSAR focus over the area of Guanshan city (close to profile 3) with a field investigation photography and a tectonic synthesis of the observed deformation.

Two field investigations have been realized (in October 2009 and May 2010) to find markers of deformations very close to this new fault trace. Figure 5 is an example of a significant thrust deformation over a dike.

To estimate precisely creep rates along the fault, a series of 50 close profiles have been calculated, like the three ones presented in Figure 5. The clear rupture in mean LOS velocity observed in each profile corresponds to the fault, and allows to localize precisely the fault line. From there, we estimate the creep rate by separating the selected PS into two subsets (both sides of the fault) and calculating the difference of velocity on both sides.

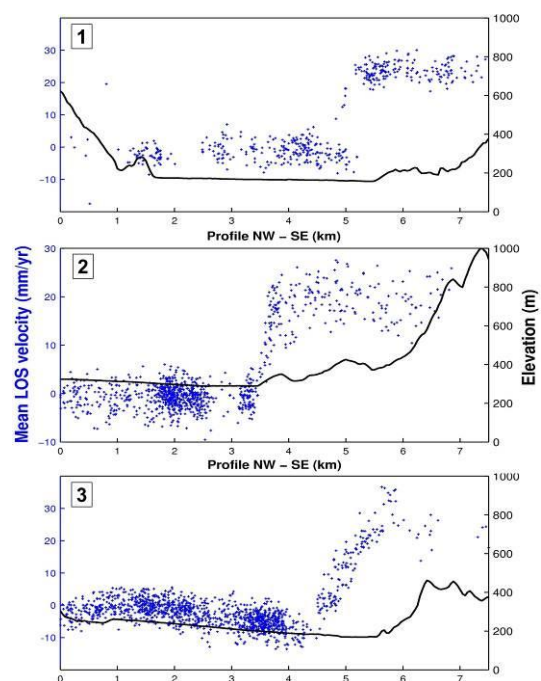


Fig. 6 Perpendicular profiles across the fault with mean LOS velocities and topography. Profiles 1, 2 and 3 are respectively located near Yuli, Chihshang and Guanshan.

Estimated creep rates are then analyzed according to the latitude to show the spatial variation of the deformation (Fig. 7A). The maximum of tectonic activity is located between Yuli and Chihshang with a 2.5 cm/yr mean LOS velocity. In order to validate these new results, we have compared them with other previous published data (InSAR ERS, leveling, GPS and creepmeters [8]).

To compare all data, we converted creep rates in LOS to dip-parallel slip assuming a fault dip angle of 45° and a look angle of 34.3° for the ALOS satellite. In a global point of view, spatial variations of dip-parallel slip from PS-InSAR are comparable with previous data. However, these new rates are globally lower than those previously published (Fig. 7B).

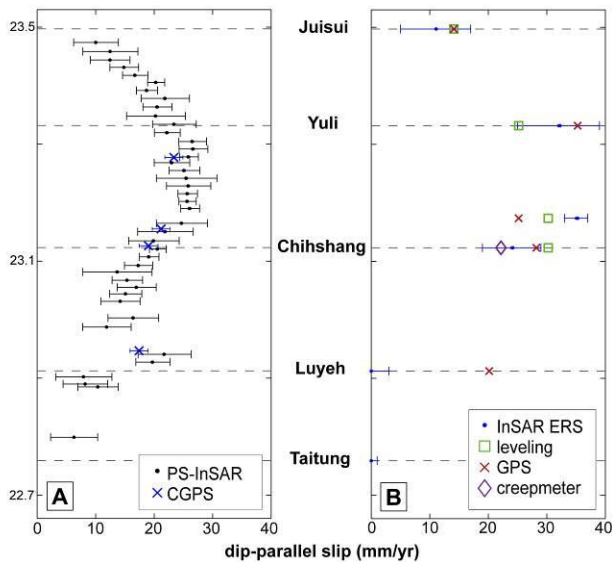


Fig. 7 (A) Spatial variation of estimated creep rates obtained from PS-InSAR. (B) Previous published data from Hsu and Bürgmann, 2006 [18].

We also compared PS-InSAR results with Continuous GPS network for the same period of study (January 2007 to February 2010). We have used 33 CGPS stations installed by different institutes (Central Weather Bureau, Academia Sinica and Ministry of Interior and National Taiwan University).

The three components of GPS displacement vector (North, East and Up) provided on each station are projected into a LOS velocity thanks to the sensitivity vector, unit vector pointing from ground to satellite and calculated by StaMPS. For each station, we selected PS within a square of 1 km by 1 km centered on the station, and calculated the mean of LOS velocities of all PS located in the square : this single mean PS value can then be compared to the GPS value..

GPS LOS velocities are plotting according to PS velocities (Fig. 8). It shows their good agreement, confirming the validity of our new PS measurements obtained with PALSAR data.

This work was the object of international and national communications [23,24,25].

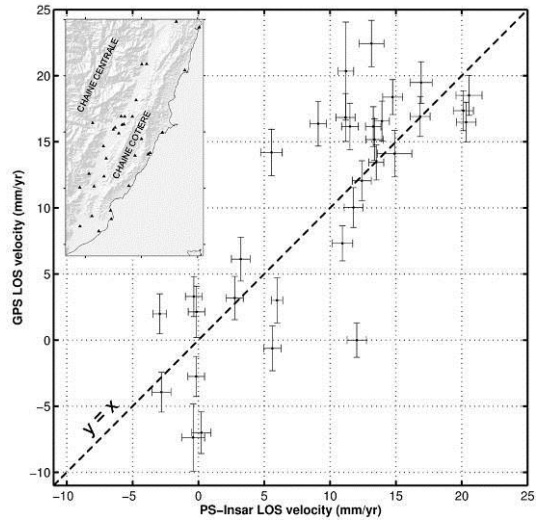


Fig. 8 Comparison between PS-InSAR velocities and CGPS velocities for the period between January 2007 and February 2010.

4. SOUTH WEST

During the first part of this project, we focused our study on the measurement and analysis of interseismic deformation in SW Taiwan (Fig. 2B). We started by the Tainan-Kaohsiung-Pingtung area because GPS and previous DINSAR studies using ERS C-Band data have shown high interseismic deformation rate in these areas associated with different processes such as anticlinal growing and fault creep [9,10,13].

We chose first the ascending track 447 which covers correctly the target area and on which they are more acquisitions than on other adjacent tracks. We ordered all available archived PALSAR images for this track, that are 17 images, acquired between January 2007 and January 2011.

A stack of 10 differential interferograms has been processed; all couples have a baseline lower than 2000m. Figure 9 shows an example of these interferograms: as expected with L-band data, the coherence of the interferograms is high on a major part of the area. Even on mountainous areas, this coherence can remain high enough for couples with time intervals up to 3-4 months.

In addition to ground displacement signal, some interferograms show clearly a phase signal related to atmospheric perturbation and orbital errors.

Signature of surface displacements is also already visible without further processing or any correction. For instance, different interferograms (such as the one in Fig. 9) show a clear signal of deformation in the SW part of the area, on the Pingtung plain. Such signal has already been observed and studied with ERS-2 images

(Fig. 9C)[12,23]. This was associated to a land subsidence, occurring specifically in dry season (no signal could be observed in wet season), and resulting from groundwater pumping for aquatic cultivation.

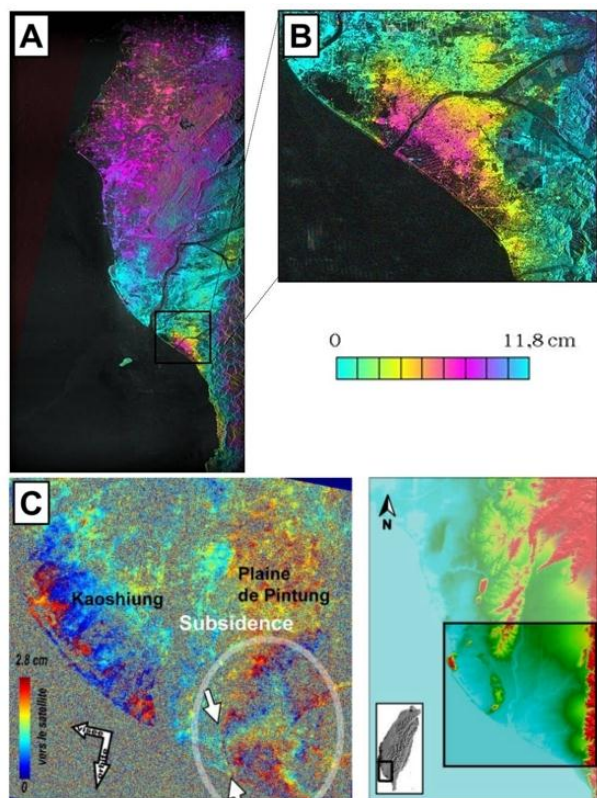


Fig. 9 (A) ALOS PALSAR interferogram on the Tainan-Kaohsiung area (July 20th 2007 - October 20th 2007). (B) Extract on Pingtung area, showing deformation signal. (C) Previous InSAR results using ERS C-band [26].

On the other hand, the detection and determination of the signal of interest, the tectonic interseismic deformation, which is of smaller amplitude, is not obvious. A more advanced analysis of interferograms has to be conducted. It will allow to correct atmospheric and orbital perturbation and to discriminate tectonic signal from pumping subsidence. This will be done through Small Baselines [1] and Persistent Scatterers approaches [2,3].

A first processing of PALSAR data using StaMPS method was realized and preliminary results are presented in Figure 10. We used 8 PALSAR data between January 2007 and July 2010. StaMPS found more than 800 000 PS over this high urbanized area, the subsidence of the Pingtung plain is clearly visible with a maximum rate of -35 mm/yr. This PS-InSAR map needs to be further analyzed, in combination with GPS measurements.

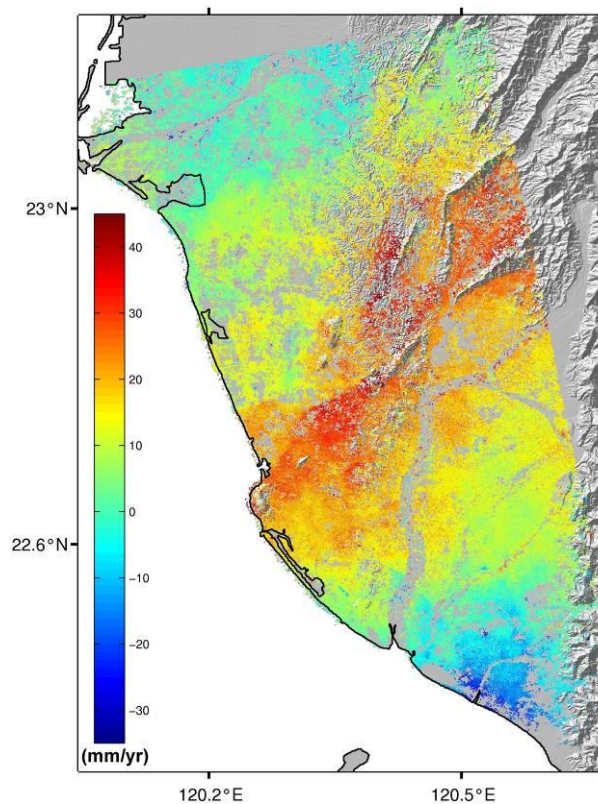


Fig. 10 PS-InSAR map of mean displacement using L-band PALSAR data obtained with StaMPS (January 2007 - July 2010).

From a methodological point of view, we have also started a comparison of different dataset in order to evaluate the respective benefit and complementarities of them, in particular PALSAR HH and HV polarization (using FBD mode) and PALSAR versus ASAR ENVISAT. To investigate the influence of the polarization on the signal quality, two interferograms have been computed with FBD images, one using HH polarization and the other using HV (Fig. 11). It appears that on our area of interest, interferogram calculated with HH polarization data leads to higher coherence that with HV polarization. This effect is more pronounced in forested area than in urban areas.

Those preliminary results are very encouraging and promising. The exploitation of these interferograms through stacking and time series for the tectonic analysis is in progress.

A comparison between PS-InSAR results from StaMPS using three dataset from different sensors (ERS, ENVISAT and ALOS) is also in progress.

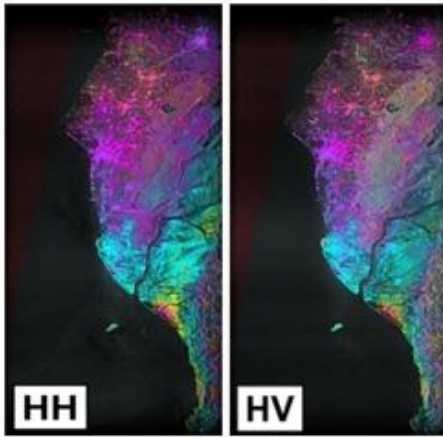


Fig. 11 Comparison of interferograms calculated with HH polarization mode (left) and with HV polarization mode (right).

5. CONCLUSION

All these works show the capacity of L-band data to increase significantly the interferometric coherence (even with important temporal baseline), contrary to C-band, and consequently the quality of both DInSAR and PS-InSAR results.

Compared to previous studies using interferometric methods with C-band SAR data, this study, combining recent PS method with new L-band data, offers an unprecedented (amazing) density of points of measurements over the Longitudinal Valley and the South West of Taiwan, improving considerably our knowledge of major active structures in Taiwan like the LVF.

Regarding the Longitudinal Valley, these results allow a new updated and precise drawing of active parts of the LVF. They give also the opportunity to study the spatial and temporal evolution of creep rates, that vary all along the fault, from south to north. For the South West, preliminary results give us new information about deformations occurring after the Chi-Chi earthquake.

All presented results lead us to continue our PALSAR data interferometric studies over Taiwan in order to increase our knowledge of interseismic deformations. However, a higher temporal frequency of acquisition is required, as it would enable to increase the accuracy of temporal evolution analysis of interseismic creep.

6. ACKNOWLEDGEMENT

We greatly appreciate the assistance of Mr Guo-Jang Jiang for the fieldwork on the Longitudinal Valley. PALSAR data were provided by the JAXA. We are also grateful to Central Weather Bureau, Academia Sinica and National Taiwan University for the GPS data.

6. REFERENCE

- [1] R. Lanari, O. Mora, M. Manunta, J.J. Mallorqui, P. Berardino & E. Sansosti, "A Small-Baseline Approach for Investigating Deformations on Full-Resolution Differential SAR Interferograms", *IEEE Transactions on Geoscience and Remote Sensing*, 42, pp. 1377-1386, 2004.
- [2] A. Ferretti, C. Prati & F. Rocca, "Permanent scatterers in SAR interferometry", *IEEE Transactions on Geosciences and Remote Sensing*, 39, pp. 8-20, 2001.
- [3] A. Hooper, P. Segall & H. Zebker, "Persistent scatterer interferometric synthetic aperture radar for crustal deformation analysis, with application to Volcán Alcedo, Galápagos", *J. Geophys. Res.*, B07407, 2007.
- [4] T. Seno, S. Stein & A.E. Gripp, "A Model for the Motion of the Philippine Sea Plate Consistent With NUVEL-1 and Geological Data", *J. Geophys. Res.*, 98, pp. 17941-17948, 1993.
- [5] S.-B. Yu & L.-C. Kuo, "Present-day crustal motion along the Longitudinal Valley Fault, eastern Taiwan", *Tectonophysics*, 333, pp. 199-217, 2001.
- [6] S.-B. Yu & C.-C. Liu, "Fault creep on the central segment of the Longitudinal Valley Fault, eastern Taiwan", *Proc. Geol. Soc. China*, 32, pp. 209-231, 1989.
- [7] J.-C. Lee, J. Angelier, H.-T. Chu, J.-C. Hu, F.-S. Jeng & R.-J. Rau, "Active fault creep variations at Chihshang, Taiwan, revealed by creep meter monitoring", *J. geophys. Res.*, 108, 2528, 2003.
- [8] L. Hsu & R. Bürgmann, "Surface creep along the Longitudinal Valley fault, Taiwan from InSAR measurements", *Geophys. Res. Lett.*, 33, L06312, 2006.
- [9] B. Fruneau, E. Pathier, D. Raymond, B. Deffontaines, C.T. Lee, H.T. Wang, J. Angelier, J.P. Rudant & C.P. Chang, "Uplift of Tainan Tableland (SW Taiwan) revealed by SAR Interferometry", *Geophys. Res. Lett.*, 28, pp. 3071-3074, 2001.
- [10] M.-H. Huang, J.-C. Hu, K.-E. Ching, R.-J. Rau, C.-S. Hsieh, E. Pathier, B. Fruneau & B. Deffontaines, "Active deformation of Tainan tableland of southwestern Taiwan based on geodetic measurements and SAR interferometry", *Tectonophysics*, 466, pp. 322-334, 2009.
- [11] C.-S. Hou, J.-C. Hu, L.-C. Shen, J.-S. Wang, C.-L. Chen, T.-C. Lai, C. Huang, Y.-R. Yang, R.-F. Chen, Y.-G. Chen & J. Angelier, "Estimation of subsidence using GPS measurements, and related hazard: the Pingtung Plain, southwestern Taiwan", *Comptes Rendus Geosciences*, 337, pp. 1184-1193, 2005.

- [12] E. Pathier, B. Fruneau, B. Deffontaines, J. Angelier, C.-P. Chang, S.-B. Yu & C.-T. Lee, "Coseismic displacements of the footwall of the Chelungpu fault caused by the 1999, Taiwan, Chi-Chi earthquake from InSAR and GPS data", *Earth and Planetary Science Letters*, 212, pp. 73-88, 2003.
- [13] J.-C. Hu, H.-T. Chu, C.-S. Hou, T.-H. Lai, R.-F. Chen & P.-F. Nien, "The contribution to tectonic subsidence by groundwater abstraction in the Pingtung area, southwestern Taiwan as determined by GPS measurements", *Quaternary International*, 147, pp. 62-69, 2006.
- [14] D. Massonnet & K.L. Feigl, "Radar interferometry and its application to changes in the Earth's surface", *Rev. Geophys.*, 36, pp. 441-500, 1998.
- [15] R. Bürgmann, P.A. Rosen & E.J. Fielding, "Synthetic Aperture Radar Interferometry to Measure Earth's Surface Topography and Its Deformation", *Annual Review of Earth and Planetary Sciences*, 28, pp. 169-209, 2000.
- [16] C.P. Chang, T.Y. Chang, C.T. Wang, C.H. Kuo & K.S. Chen, "Land-surface deformation corresponding to seasonal ground-water fluctuation, determining by SAR interferometry in the SW Taiwan", *Mathematics and Computers in Simulation*, 67, pp. 351-359, 2004.
- [17] P.A. Rosen, S. Hensley, G. Peltzer & M. Simons, "Updated Repeat Orbit Interferometry package released", *Eos Trans. AGU*, 85, pp. 35, 2004.
- [18] H. Zebker & J. Villasenor, "Decorrelation in Interferometric Radar Echoes", *IEEE Transactions on Geosciences and Remote Sensing*, 30, pp. 950-959, 1992.
- [19] B. Kampes & S. Usai. "Doris: The Delft Object-oriented Radar Interferometric software", *Proceedings ITC 2nd ORS symposium*, 1999.
- [20] C.W. Chen & H.A. Zebker, "Network approaches to two-dimensional phase unwrapping: intractability and two new algorithms", *J. Opt. Soc. Am. A*, 17, pp. 401-414, 2000.
- [21] J.B.H. Shyu, L.-H. Chung, Y.-G. Chen, J.-C. Lee & K. Sieh, "Reevaluation of the surface ruptures of the November 1951 earthquake series in eastern Taiwan, and its neotectonic implications", *J. of Asian Earth Sciences*, 31, pp. 317-331, 2007.
- [22] J.-C. Hu, L.-W. Cheng, H.-Y. Chen, Y.-M. Wu, J.-C. Lee, Y.-G. Chen, K.-C. Lin, R.-J. Rau, H. Kuo Chen, H.-H. Chen, S.-B. Yu & J. Angelier, 2007. "Coseismic deformation revealed by inversion of strong motion and GPS data: the 2003 Chengkung earthquake in eastern Taiwan", *Geophys. J Int.*, 169, pp. 667-674, 2007.
- [23] E. Pathier, J. Champenois, B. Fruneau, B. Deffontaines, K.-C. Lin & J.-C. Hu, "New observations of the Longitudinal Valley Fault creep (Taiwan) from PS-INSAR using ALOS data", *4th Joint PI Symposium of ALOS Data Nodes for ALOS Science Program*, Tokyo, November 2010.
- [24] J. Champenois, B. Fruneau, E. Pathier, B. Deffontaines, K.-C. Lin & J.-C. Hu, "Persistent Scatterer InSAR with ALOS data applied to the monitoring of the Longitudinal Valley fault (Taiwan)", *Geodynamics and Environment in East Asia International Conference & 6th Taiwan-France Earth Sciences Symposium*, Aix-en-Provence, July 2010.
- [25] J. Champenois, B. Fruneau, E. Pathier, B. Deffontaines, K.-C. Lin & J.-C. Hu, "Etude de la tectonique active de Taiwan par Interférométrie Radar et Réflecteurs Permanents, Exemple de la Vallée Longitudinale", *Colloque annuel du Comité National de Géodésie et Géophysique*, Le Mans, November 2010.
- [26] E. Pathier, "Apports de l'interferometrie radar differentielle a l'etude de la tectonique active de Taiwan", *Ph.D. Thesis, Universite Marne-La-Vallee, Paris, France*, 273 pp, 2003.